IEEE Access
Multidisciplinary | Rapid Review | Open Access Journal

SPECIAL SECTION ON ARTIFICIAL INTELLIGENCE TECHNOLOGIES FOR ELECTRIC POWER SYSTEMS

Received July 26, 2019, accepted August 12, 2019, date of publication August 19, 2019, date of current version August 31, 2019.

Digital Object Identifier 10.1109/ACCESS.2019.2936212

A Novel Intuitionistic Fuzzy Inhibitor Arc Petri Net With Error Back Propagation Algorithm and Application in Fault Diagnosis

MINGYUE TAN, JIMING LI, GUANGYUAN XU, AND XUEZHEN CHENG, (Member, IEEE)
Department of Electrical Engineering and Automation, Shandong University of Science and Technology, Qingdao 266590, China
Corresponding author: Xuezhen Cheng (zhenxc6411@163.com)

Mingyue Tan and Jiming Li contributed equally to this work.

This work was supported in part by the National Natural Science Foundation of China under Grant 61503224, in part by the Shandong Natural Science Foundation of China under Grant ZR2017MF048, in part by the Shandong Province Graduate Education Quality Improvement Plan Construction Project under Grant 2016050, in part by the Qingdao Minsheng Science and Technology Plan Project under Grant 17-3-3-88-nsh, and in part by the Shandong University of Science and Technology Postgraduate Innovation Program under Grant SDKDYC180232.

ABSTRACT The setting and adjustment of the weight parameters in the traditional fault diagnosis method depend entirely on personal experience, and the parameter setting lacks regularity. To reduce the fault diagnosis errors caused by human subjective factors and improve the speed and accuracy of power grid fault diagnosis, we propose a method for power grid fault diagnosis using intuitionistic fuzzy inhibitor arc Petri net (IFIAPN) with error back propagation (BP) algorithm. Firstly, according to the network topology analysis and relay protection configuration setting rules, the inhibitor arc (IA) tuple is introduced into the model structure of the intuitionistic fuzzy Petri net to reduce the ambiguity of protection and circuit breaker action. Then, the weight parameters in the model are trained using a BP neural network algorithm to enhance the objectivity of the parameters. Finally, a simulation of an IEEE-39 node system and a real case study using the Hou-zhong line local grid were used to verify the effectiveness of the fault diagnosis method. The results show that the method can effectively deal with the refusal and mis-operation of multiple circuit breakers and improve the diagnostic efficiency under complex data environment.

INDEX TERMS Intuitionistic fuzzy set, inhibitor arc Petri net, BP algorithm, grid fault diagnosis.

I. INTRODUCTION

As the scale of the power grid continues to expand and the number of renewable power integrations [1] continues to increase, the complexity of faults increases, which significantly increases the difficulty of power grid fault diagnosis.

The application of smart grid fault diagnosis provides technical support for constructing real-time and reliable online power grid fault diagnosis systems. At present, the main grid intelligent fault diagnosis methods include: Expert systems [2], Bayesian networks [3], Artificial neural networks (ANNs) [4], Fuzzy analysis [5], Petri net (PN) [6], and some combination methods [7]. In recent years, fuzzy Petri net (FPN) has attracted considerable attention in grid fault diagnosis applications due to being simple, fast, and concurrent. Based on the current status quo, the research on Petri net fault diagnosis methods mainly covers two aspects: optimization of models and algorithms, and information processing.

In terms of optimization of models and algorithms, given the inability of the Petri net model to adapt to changes in the network topology, some research has devised corresponding solutions. A grid fault diagnosis method based on directional weighted fuzzy Petri net was proposed in Yang *et al.* [8]; the various propagation directions of electrical equipment (Eq) faults were separately modeled and weighted, which improved the flexibility and adaptability of the diagnostic model. Xie and Tong [9] proposed a grid fault diagnosis method based on hierarchically transition Petri net, which reduces the matrix dimension and avoids repeated modeling when the network topology changes. To reduce the order of the association matrix, Li *et al.* [10] introduced the association matrix reduction technique, and then deleted the Place unrelated to the reasoning. The calculation amount was reduced, which improved the efficiency of fault diagnosis.

The associate editor coordinating the review of this article and approving it for publication was Canbing Li.

From the perspective of information processing, improving the effective use of alarm information is essential to improving the accuracy of fault diagnosis. To improve the processing ability of uncertain information, a Petri net fault diagnosis method based on probability information was studied [11]. The combination of FPN and probability information has better processing ability for uncertain information in the power grid. To fully use the alarm information and reduce the uncertainty of the information, a power grid fault diagnosis method based on the intuitionistic fuzzy Petri net was proposed, which enhances the description of the alarm information by considering the membership degree and non-membership degree of the information [12]. In [13], the time series information was introduced into Petri net power grid fault diagnosis, which was able to filter some uncertainty information and correct the error information, thereby further improving the accuracy of the fault diagnosis. In addition, the reasoning process based on matrix operations is given in this method, which makes the calculations more concise and efficient. With the continuous development of Petri net in the field of fault diagnosis, the current and future research trends of Petri net fault diagnosis mainly involve exploring the combination of multi-source data fusion [14], [15] and neural networks [16] to solve the uncertainty of information and improve the diagnostic speed in complex data environment. A novel approach to pattern classification using a concept of fuzzy Petri nets was proposed [17], which introduced the neural structure of the FPN and provided details of the learning algorithm and illustrative digital experiments.

The above grid fault diagnosis methods for fuzzy Petri net have achieved improved the accuracy of fault diagnosis results, the fault tolerance of the model, and the speed of diagnosis. However, these models do not adequately embody the logical relationship of relay protection in the model structure and differ from the actual situation. Hierarchical modeling of Eq solves the matrix dimension increase problem to a certain extent, but the model needs to be rebuilt when the network topology changes. The setting of parameters in the field of grid fault diagnosis depends largely on expert experience and theoretical support is lacking, which makes the diagnosis results susceptible to subjective factors. Given these problems, the improvements and advantages of the method proposed in this article are as follows: A novel method of intuitionistic fuzzy inhibitor arc Petri net is used to construct the model of power grid (IEEE-39 node system). Experiential data and the back propagation (BP) algorithm in neural net are used to train the weight parameters in the model to improve diagnosis accuracy. Using layered transition technology to improve the adaptability and flexibility of the model, the value of the membership degree and the non-membership degree are optimized separately during the inter-layer calculation.

The validity of the proposed method was verified with a case simulation of the IEEE-39 node system and a real case using the Hou-zhong line local grid.

II. INTUITIONISTIC FUZZY PETRI NET WITH INHIBITOR ARC

A. BASIC THEORY OF INTUITIONISTIC FUZZY SET

The characteristic of intuitionistic fuzzy set [18] considers both the membership and non-membership information simultaneously, which provides more options in the description of the attributes of things, and has stronger performance when dealing with uncertain information. The intuitionistic fuzzy set is defined according to Liu *et al.* [19] as follows:

Definition 1: Assuming X is a given theoretical domain, the definition of the intuitionistic fuzzy set in the domain X is as follows:

$$A = \{\langle \mu_A(x) + \gamma_A(x)\rangle | x \epsilon X\}$$

(1) $0 \leq \mu_A(x) + \gamma_A(x) \leq 1$, where $\mu_A(\mathrm{x}) :\rightarrow [0, 1]$ and $\gamma_A(\mathrm{x}) :\rightarrow [0, 1]$ are respectively the membership function and the non-membership function of the set A. For any element in set A, if $x \epsilon X$, then $0 \leq \mu_A(x) + \gamma_A(x) \leq 1$.

(2) The function pair $(\mu_A(x), \gamma_A(x))$ is defined as the intuitionistic fuzzy index in the X domain, which is composed of membership degree $\mu_A(x)$ and non-membership degree $\gamma_A(x)$.

(3) Set $A = \{\langle x, \mu_A(x), 1 - \mu_A(x)\rangle | x \epsilon X\}$ as the degree of hesitation of x in the intuitionistic fuzzy set A, and the domain of X, $\mu_A(x)$ reflecting the degree of certainty of event occurrence, $\gamma_A(x)$ reflecting the degree of uncertainty of event occurrence, and x belongs to the set A. If $\forall x \epsilon X$, then $0 \leq \pi_A(x) \leq 1$.

B. PETRI NET WITH INHIBITOR ARC

The Petri net with inhibitor arc [20] is formed by adding an arc connecting the place and transition on the basis of the original Petri net. As shown in Figure 1, *IA* indicates the inhibitor arc. transition T cannot fire when there is a token in Place P_1, but transition T can fire when there is no token in Place P_1. This arc only controls the transition that meets the enabling condition. After the transition firing, the inhibitory arc does not have any influence on the resulting identity change.

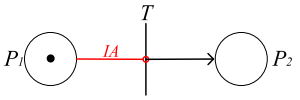

FIGURE 1. Inhibitor arc model.

Definition 2: Petri net with inhibitor arc is a five-tuple $\sum = \{S, T, F, I, M\}$, $\{S, T, F\}$ is a network, and M is an identifier of the network, $I \subset S \times T$ is called a collection of inhibitor arc $I \cap F = \phi$, (scilicet $\forall s \in S \wedge \forall t \in T : (s, t) \in F \rightarrow (s, t) \notin I$), for $t \in T$, $\forall s \in S : (s, t) \in F \rightarrow M(s) \geq 1$, $\forall s \in S : (s, t) \in I \rightarrow M(s) = 0$, then t fires in the M state (referred to as $M[t>$); if $M[t>$, then the transition t firing

under M state to generate a new identity M':

$$M' = \begin{cases} M(s) - 1, & IF\ (s,t) \in F \wedge (t,s) \notin F \\ M(s) + 1, & IF\ (s,t) \in F \wedge (t,s) \notin F \\ M(s), & others \end{cases} \quad (1)$$

C. DEFINITION OF IFIAPN

Definition 3: Intuitionistic Fuzzy Petri net with Inhibitor Arc is an eight-tuple.

$$\text{IFIAPN} = \{P, T_\lambda, F, S, U, I, O, M_0\}$$

(1) $P = \{p_1, p_2, p_3, \ldots, p_n\}$ indicates a collection of finite place in IFIAPN.

(2) $T_\lambda = \{\lambda_1, \lambda_2, \lambda_3, \ldots, \lambda_n\}$ indicates a set of finite transitions in IFIAPN.

(3) $F = \{f_1, f_2, f_3, \ldots, f_n\}$ indicates a set of transition domain values in IFIAPN; $f_j = (\mu_{tj}, \gamma_{tj}), j = 1, 2, 3, \ldots, m$ is intuitionistic fuzzy set; $\mu_{tj} \geq 0$ and $\gamma_{tj} \geq 0$ respectively represent the certainty and uncertainty of transition λ_j.

(4) $S = \{s_1, s_2, s_3, \ldots, s_n\}$ indicates the initial place with inhibitor arc.

(5) $U = \{u_1, u_2, u_3, \ldots, u_n\}$ indicates the transition firing matrix of each step. When each step has a transition firing, the transition value is set to 1; otherwise, it is zero. When the step is completed, the matrix returns to the initial state, and then the corresponding operation is performed when transition firing.

(6) I represents the input matrix $I = (W_{Iij})_{n\times m}$; W_{Iij} represents the logic element; and $W_{Iij} \in [0, 1]$ and $\sum_{0\leq i\leq n} W_{Iij} = 1$. If there is a directed arc from p_i to transition t_i, then the value of W_{Iij} is the weight of the directed arc. If there is no directed arc from p_i to t_i, then $W_{Iij} = 0$, $i = 1, 2, 3, \ldots, n; j = 1, 2, 3, \ldots, m$.

D. DEFINITION OF OPERATORS

In the algebraic matrix, to facilitate algorithmic reasoning, the following operators are defined:

Suppose A, B, and C are all m × n order matrices, D is m × q matrix, and E is a q × n matrix.

(1) Direct multiplication operator $\cdot$: $C = D \cdot E$, that is, $c_{ij} = a_{ij}b_{ij}$

(2) Comparison operator $\odot$: $C = A \odot B$, that is, $c_{ij} = (1, 0)$, when $a_{ij} \geq b_{ij}$; otherwise, $c_{ij} = (0, 1)$.

(3) Multiplication operator $\otimes$: $C = D \otimes E, c_{ij} = \max_{1\leq k\leq q} (d_{ik}q_{kj})$

(4) Addition operator $\otimes$: $C = A \otimes B$, $c_{ij} = \max(a_{ij}, b_{ij})$.

III. IFIAPN POWER GRID FAULT DIAGNOSIS METHOD

The traditional power grid fault diagnosis method will considerably reduce the speed of obtaining diagnostic results when a large number of calculations are required under complex fault conditions, which will affect the real-time performance of fault diagnosis. The parameters set based on traditional experience make the diagnosis results susceptible to human factors. The artificial setting of weight parameters depends entirely on personal experience, and there is no regularity in parameter adjustment. Such parameters are not universal and lack theoretical support.

Aiming to solve the above problems, the IFIAPN fault diagnosis model is built in this section and the BP algorithm is used to train the weight parameters of the IFIAPN model. The whole reasoning process of the method mainly includes two parts: forward and backward reasoning.

As shown in Figure 2, the whole reasoning process of the method is as follows:

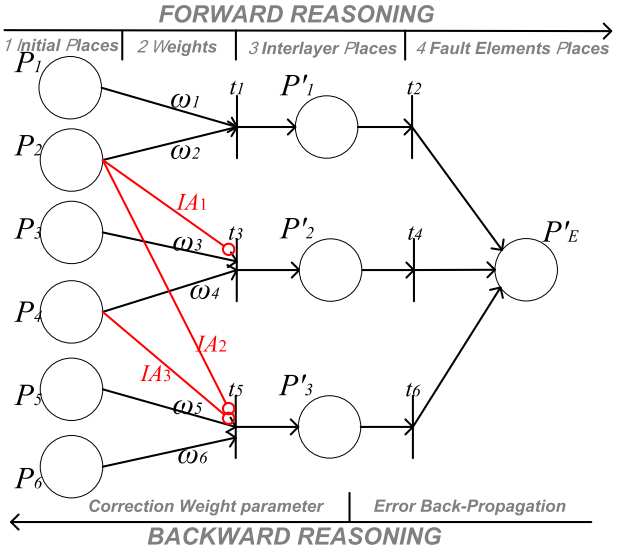

FIGURE 2. Algorithm structure diagram.

(1) When the grid fails, the dispatch center receives a large amount of alarm information, the suspicious fault Eq can be obtained according to the alarm information, and the sets of suspicious fault Eq can be constructed.

(2) Establish the IFIAPN fault diagnosis model for the suspected fault Eq, and assign the probability value of the initial Places, where the action component is represented by the Place containing the token. As shown in Figure 2, if there are tokens in the P_1 and P_2 locations, then transition t_1 can be enabled and transitions t_3 and t_5 cannot be enabled.

(3) In the process of forward reasoning, the membership value of confidence is optimized in "3 Interlayer Place" (Figure 2), the non-membership value is optimized in "4 fault element positions" (Figure 2), and finally, the fault probability value of Ep is obtained.

(4) In the backward reasoning process, the action state of the corresponding protection and the circuit breaker can be inferred according to the faulty device. Using the error back propagation algorithm, the weight of "2 Weights" (Figure 2) in the forward reasoning process can be trained so that forward reasoning can produce better fault diagnosis results.

A. MODELING OF IFIAPN

To fully reflect the advantages of model structure in fault handling, reduce the amount of calculation, and meet the

requirements of real-time online fault diagnosis, we introduce the inhibitor arc into the Petri net structure, and embed the action logic of the relay protection in the model structure.

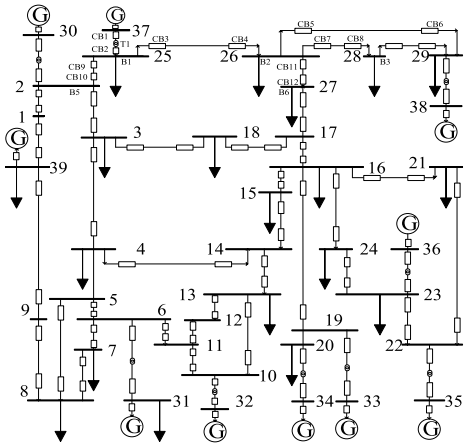

FIGURE 3. IEEE-39 node system diagram.

The IEEE-39 node system diagram is shown in Figure 3 and the IFIAPN fault diagnosis model of the Busbar B_1 is shown in Figure 4. (μ_1, γ_1) is the identification value for place P_1, μ_1 and γ_1 respectively represent the certainty and the uncertainty of P_1, (μ_{t1}, γ_{t1}) is the threshold value for transition t_1, and (μ_{t2}, γ_{t2}) is the identification value for the output arc from t_3.

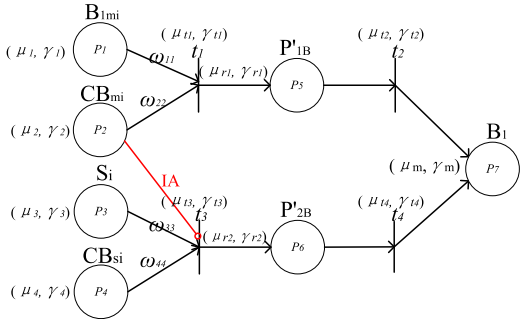

FIGURE 4. General basic model of the Busbar.

B_{1mi} represents the main protection Place P_1 of the Busbar B_1, and CB_{mi} represents the corresponding circuit breaker Place P_2. S_i represents the remote backup protection Place P_3 of B_1, and CB_{si} represents the corresponding circuit breaker Place P_4. ω_{11}, ω_{33} and ω_{22}, ω_{44} indicate the degree of influence of the protection device and the corresponding circuit breaker on the fault diagnosis, respectively. t_1, t_2, t_3, and t_4 are transitions, the transition threshold (μ_{tj}, γ_{tj}) were set to (0.2, 0.7) according to Zhang *et al.* [12]. *IA* is the inhibitor arc. When the token exists in the CB_{mi} Place, the transition t_2 cannot fire. P'_{1B} and P'_{2B} represent virtual Places P_5 and P_6, respectively. The identification value of the output directed arc is (1, 0). The initial value of the front-end Eq Place and the inter-layer Place is (0, 1). (μ_{r1}, γ_{r1}) and (μ_{t2}, γ_{t2}) indicate the degree of influence of the main protection devices and their circuit breaker devices on the fault diagnosis results, respectively; and (μ_m, γ_m), indicates the degree of support from transitions t_2 and t_4 to the device Place P_7, with a value of (0.95, 0.025).

When Busbar B_1 fails, if the main protection B_{1m} and the corresponding circuit breaker CB_{mi} are cut off due to the existence of the IA, the transition t_3 for the backup protection of B_1 cannot fire, and the corresponding remote backup cannot be operated. If CB_{mi}, corresponding to the main protection refuses to trip, transition t_3 fires. At this time, the corresponding remote backup protection and its circuit breaker are used for fault deduction. In this case, only the triggered protection device and the tripped circuit breaker participate in the failure probability calculation, and the untriggered protection device and the circuit breaker, without tripping, do not participate in the failure probability calculation, which causes the calculation result to be significantly lower. Since the logical relationship is defined in the structure, the judgment of the structural logic is faster than the fuzzy processing of the algorithm logic.

In order to meet the requirements of modeling large-scale grid faults, enhance the flexibility of the model, this paper adopts the form of hierarchical modeling on the model structure. When the network topology changes, only the confidence of the initial library in the direction of the fault propagation of the first layer needs to be updated. There is no need to increase or decrease the branch structure, which enhances the adaptability and flexibility of the model. In the first layer model, a two-layer transition structure is adopted.

This model has a good ability to judge the protection and circuit breaker's refusal and mis-operation. Taking the Busbar model in Figure 4 as an example, if a CB_{mi} trip error occurs, the transition of the corresponding backup protection of the Busbar cannot fire, the final probability value of the calculated Busbar is relatively small, and CB_{mi} is more likely to be judged as a trip error. According to the protection setting rules, if the CB_{mi} refuses tripping, the corresponding backup protection starts because there is no token in the input Place connected via the inhibitor arc, so the corresponding Busbar backup protection transition fires. Depending on the combination of Eq that acts on the trip, the Eq that refuse operation can be quickly determined. The computation amount in the improved model is significantly reduced, especially in the event of a complex fault, since it only needs to calculate the probability value of the direction of the trip element without the need for all calculations.

B. FORWARD REASONING

After the IFIAPN fault diagnosis model of the Eq is established, the degree of membership and non-membership of the equipment can be calculated using the inference algorithm described below.

To improve the accuracy of the fault diagnosis results, Tan *et al.* [13] used the intuitionistic fuzzy Petri net fault diagnosis method, and the Gaussian function was used to optimize the fault probability value. The IFIAPN fault diagnosis

method in this paper considers two aspects: membership degree and non-membership degree. If the two aspects of intuitionistic fuzzy set can be optimized simultaneously, the accuracy of the fault diagnosis result results can be further improved, so the algorithm is optimized as follows.

1) ALGORITHM OPTIMIZATION FOR MEMBERSHIP DEGREE

$$\psi_u^k = f_\psi(O_{n\times 1}^k \otimes \psi_{\mu m\times 1}^{k-1}) \tag{2}$$

The deterministic value of the inter-layer identification value is processed by a Gaussian function and applied to the matrix derivation process, where ψ indicates identification value, ψ_μ represents the identification value of the membership degree, and $f_\psi(x)$ is a Gaussian function [13]:

$$f_\psi(x) = e^{-3(x-1)^2} \tag{3}$$

The application of this function can better align the calculation results with the characteristics of fault diagnosis and ensure the probability of failure is more likely to be the ideal final value within (0, 1).

As shown in Figure 4, for the main protection of B_1 and the corresponding circuit breaker action trip, the calculated probability value between layers is (0.8459, 0.01091), and the probability value after processing via Gaussian function is $f(P'_{1B}) = (0.9312, 0.01091)$. The degree of certainty of the probability is more in line with the algorithm requirements.

2) ALGORITHM OPTIMIZATION FOR NON-MEMBERSHIP DEGREE

$$\psi_\gamma^k = \gamma'_\psi(O_{n\times 1}^k \otimes \psi_{\gamma m\times 1}^k) \tag{4}$$

For a faulty Eq in the system, when the primary protection of the Eq or the corresponding circuit breaker refuses to trip, the backup protection of the Eq corresponding to the direction in which the fault propagates will trip to remove the fault. The greater fault protection and the number of circuit breakers for the tripping of the faulty Eq in the direction of the fault propagation prove that the greater the probability of failure of the Eq, the less the uncertainty of the corresponding Eq fault. Based on this theory, the non-membership degree value of the terminal Place in the direction in which the faulty element propagates is corrected to Equation (4). ψ_γ represents the identification value of the non-membership degree. The definition of γ'_ψ is as follows. If the number of propagation directions of the faulty Eq after the analysis is *Num*, the non-membership degree of the terminal Place in the Eq failure propagation direction is γ, and the value of the non-membership degree after the correction is γ'_ψ, then:

$$\gamma'_\psi = \frac{\gamma}{Num} \tag{5}$$

The final identification value after correction is:

$$\psi_{m\times 1}^k = (\psi_u^k, \psi_\gamma^k) \tag{6}$$

The measurement function of the fault probability of the device is:

$$f(N) = \begin{cases} \dfrac{\psi_u^k - \psi_\gamma^k}{\psi_u^k}, & \psi_u^k > \psi_\gamma^k \\ 0, & \psi_u^k < \psi_\gamma^k \end{cases} \tag{7}$$

where N represents the faulty device and $f(N)$ is the probability value of the faulty device. When the measured value of the failed component is $f(N) > \theta$, the electrical device N is determined to be the faulty electrical device, wherein θ is the threshold of the electrical device N failure, which is set to 0.75.

3) REASONING RULE OF IFIAPN

Calculation process of the algorithm of power grid fault diagnosis is illustrated in Figure 5, the matrix reasoning rule of IFIAPN is as follows.

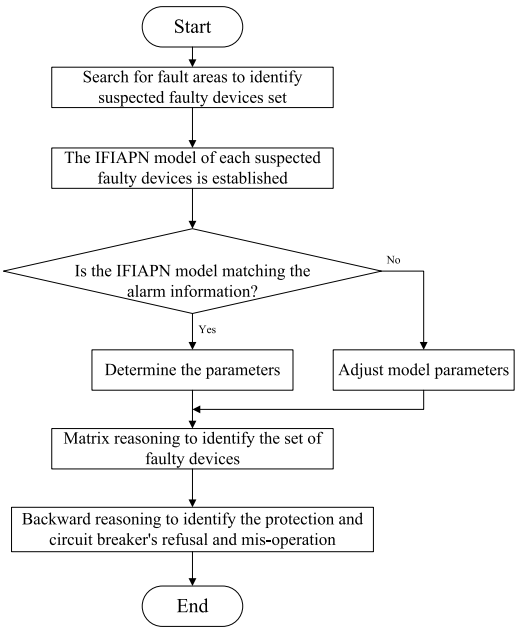

FIGURE 5. Calculation process of the algorithm curve.

(1) Calculate the input intuitionistic fuzzy value of the transition.

$$\eta_{m\times 1}^k = I_{n\times m}^T \cdot M_{n\times 1}^k \tag{8}$$

(2) Let Q be the inhibitor arc set, compare the transition domain value with the input intuitionistic fuzzy value, and at the same time, satisfy the front-end Place of the inhibitor arc of the transition to be zero, or no inhibitor arc is connected to the transition. $\neg Q$ indicates that the identifier of the front-end Place of the inhibitor arc is 0, and a transition set $\varphi_{m\times 1}^k$ that the transition firing can be obtained by the following equation.

$$\varphi_{m\times 1}^k = {}^\neg Q \wedge \eta_{m\times 1}^k \odot F_{m\times 1} \tag{9}$$

(3) Calculate the input intuitionistic fuzzy value that can fire the transition, according to the obtained set $\varphi_{m\times 1}^k$ of

transitions that can be fired.

$$\psi^k_{m\times 1} = \eta^k_{m\times 1} \cdot \varphi^k_{m\times 1} \tag{10}$$

(4) Calculate the discriminant value of the place $M^{k+1}_{n\times 1}$ obtained by $k+1$ calculations.

$$M^{k+1}_{n\times 1} = O^k_{n\times 1} \otimes \psi^k_{m\times 1} \oplus M^k_{n\times 1} \tag{11}$$

(5) If $M^{k+1}_{n\times 1} = M^k_{n\times 1}$, then the identification value matrix of the Petri net is stable, that is, the reasoning ends otherwise, let $k = k+1$, and return to step (1).

C. BACK PROPAGATION TRAINING

During the whole forward reasoning process, the degree of influence of different Eq Place on the fault diagnosis results is different, which is expressed in the model as the output weight of the initial Place.

The weight training steps of the IFIAPN model are as follows:

(1) Initialize the weight parameters that need to be learned.

(2) Input N set of samples in turn, calculate the error of the output layer, and correct the weight of the model by means of error BP.

(3) When the error meets the allowable range, the study ends, otherwise it enters the next round of training.

Due to the structural and formal of Petri net model are similar to the BP neural network model [17], the BP idea was introduced into the IFIAPN model to train the weight parameters of the IFIAPN model

We mainly trained the weight parameters of the Place corresponding to the following Eq in the model: the weight parameters of the Busbar (the main protection, the circuit breaker of the main protection, the remote backup protection, and the circuit breaker of the remote backup protection); and the weight parameters of the line and transformer (the main protection, the circuit breaker of the main protection, the near backup protection, the circuit breaker of the near backup protection, the remote backup protection, and the circuit breaker of the remote backup protection). Table 1 lists the initial values of the parameter weights of the Busbar.

TABLE 1. Initial weights of the parameters.

Parameter	Initial value	Parameter	Initial value
ω_{11}	0.3	ω_{33}	0.75
ω_{22}	0.7	ω_{44}	0.25

The reasoning process uses the official statistical probability data from 2006 to 2015 [22], [23]. In addition, the total numbers of permutation combinations of the initial P_1, P_2, P_3, and P_4 corresponding action information in the IFIAPN model of the Busbar are also determined. There are two inputs and one output in the training. The two inputs represent the input confidence of the protection and circuit breaker respectively. The output is the probability of the faulty device. According to the network model of B_1 shown in Figure 4, the signal generated under multiple types of faults is used as a fault set of the Busbar for training the entire network.

The part based on the BP algorithm is as follows. The quadratic error function for the input mode pair for each sample p is:

$$J_p = \frac{1}{2}\sum\nolimits_{n=1}^{N} (d^p_n - f^p_n)^2 \tag{12}$$

The total error function of the N training samples in the system is:

$$J = \sum\nolimits_{p=1}^{M} J_p = \frac{1}{2}\sum\nolimits_{p=1}^{M}\sum\nolimits_{n=1}^{N} (d^p_n - f^p_n)^2 \tag{13}$$

According to the gradient descent method, the weight correction amount in batch processing is:

$$\omega_{ij}(k+1) = \Delta\omega_{ij} + \omega_{ij}(k) \tag{14}$$

$$\Delta\omega_{ij} = -\eta\frac{\partial J}{\partial \omega_{ij}} \tag{15}$$

According to the chain derivatives rules:

$$\left(\frac{\partial J}{\partial \omega_{ij}}\right)^p = \frac{\partial J}{\partial f}\frac{\partial f}{\partial An_{ki}}\frac{\partial An_{ki}}{\partial O_i}\frac{\partial O_i}{\partial An_j}\frac{\partial An_j}{\partial \omega_{ij}} \tag{16}$$

where $n_j = \sum_{i=1}^{m}(x_i\omega_{ij})\partial An_j = \sum\limits_{i=1}^{m}(x_i\omega_{ij})$, O_i is the output of the i-th neuron in the hidden layer, $\partial An_j = O_i\omega_{ki}$, $(\omega_{ki} = 1)$, and η represents the learning rate.

D. SIMULATION

We used cross-validation to verify the effectiveness of the proposed method. The data were divided into a training set and a test set. First, the weight set parameter of the model was trained using the training set and verified with the test set. Then, we repeated the above process by reselecting the training set and test set. Finally, we used the loss function to evaluate and select the optimal model and parameters.

In the process of k-fold cross validation, the original data are randomly divided into k parts without repeated sampling, one of which is selected as the test set, and the remaining k-1 are used as the training set for model training. The process is repeated k times so that each subset has an opportunity to serve as a test set and the remaining opportunities as a training set. In the training process of IFIAPN, the learning rate η was 0.02, and the learning was repeated 20,000 times.

After training on each training set, a model is obtained, which is tested on the corresponding test set. The average errors of the k-fold cross validation results are shown in TABLE 2 (k = 9).

Group 1 was selected as the training model to determine the weight parameters. The weight convergence curve and the error convergence curve are shown in Figure 6. The training process for each of the transformer and the line that requires correction of the weight parameter is similar to the Busbar, so the correlation convergence curve is not listed here.

The weight parameters were trained and finally converged to fixed values, as shown in Table 3. In the actual situation, the

TABLE 2. Parameters of average error.

Group number	Average error	Group number	Average error
1	1.7876×10^{-4}	5	2.0972×10^{-4}
2	1.8211×10^{-4}	6	2.0506×10^{-4}
3	1.7549×10^{-4}	7	1.5343×10^{-5}
4	1.7432×10^{-4}	8	1.7873×10^{-5}

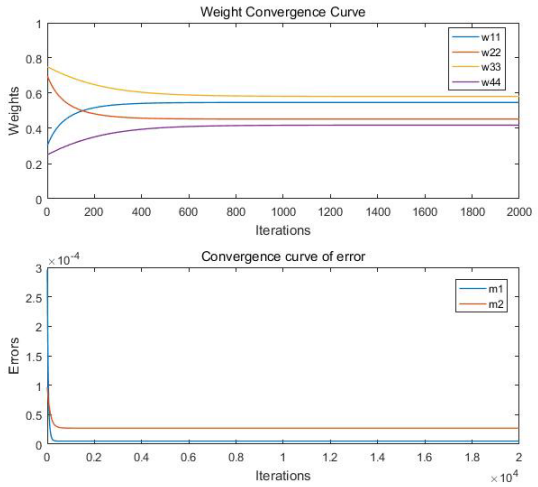

FIGURE 6. Weight and error convergence curve.

TABLE 3. Parameters after neural network training.

Protection / Eq	Main protection	Near backup protection	Remote backup protection
Transmission line	0.5096	0.6061	0.6013
Circuit breaker	0.4904	0.3939	0.3987
Transformer	0.5951	0.5733	0.6013
Circuit breaker	0.4049	0.4267	0.3987
Busbar	0.5473	--	0.5817
Circuit breaker	0.4527	--	0.4183

circuit breaker trips because the protection has been activated (normal), so the weight of the protection should be greater than the weight of the circuit breaker. The weight parameters after training fully meet this requirement, which proves that the convergence data obtained in this paper is in line with the actual situation.

To verify the validity of the determined parameters, six sets of test data were randomly selected for calculation verification. The results are compared shown in Table 4.

TABLE 4. Test set verification result.

Test set		Expected value	Calculated value	Error
0.2000	0.2000	0.1500	0.1466	0.0034
0.7000	0.7449	0.8000	0.7908	0.0092
0.6409	0.7420	0.7500	0.7447	0.0053
0.9831	1.0000	0.9900	0.9997	0.0097
0.9832	0.2000	0.7000	0.7004	0.0004
0.9792	1.0000	0.9900	0.9995	0. 0095

The difference between the calculated and expected values of the randomly selected six sets of test sets was small, which verified the effectiveness of the training meaning that the corresponding reasonable output can be provided for the input that is not the sample data.

To clarify the algorithm reasoning process presented in this paper, take the busbar B_1 fault (the main protection and the corresponding circuit breaker all correctly trip) as an example. The fault confidence of B_1 in the T_1 direction is calculated in matrix form and the final failure probability of B_1 is obtained. The identification value of the initial Place is shown in [12].

The case deduction process is as follows:

1) For input matrix$I$ with weights:

$$I = \begin{bmatrix} 0.5473 & 0.4527 & 0 & 0 & 0 & 0 & 0 \\ 0 & 0 & 0.5817 & 0.4183 & 0 & 0 & 0 \\ 0 & 0 & 0 & 0 & 1 & 0 & 0 \\ 0 & 0 & 0 & 0 & 0 & 1 & 0 \end{bmatrix}$$

The weight parameters used in the matrix are those that have been fixed after training.

2) Output matrix O with identification value, shown at the bottom of this page.

3) The matrix of transition thresholds:

$$\Gamma = [(0.2, 0.7)(0.2, 0.7)(0.2, 0.7) \\ (0.2, 0.7)(0.2, 0.7)(0.2, 0.7)]$$

4) The matrix of the fuzzy value of the initial Place and its iterative matrix are:

$$M_0 = [(0.8564, 0.01158), (0.8333, 0.00965), \\ (0.13702, 0.0724), (0.1417, 0.0568), \\ (0, 1), (0, 1), (0, 1)]$$

$$M_1 = [(0.8564, 0.01158), (0.8333, 0.00965), \\ (0.13702, 0.0724), (0.1417, 0.0568), \\ (0.9312, 0.01071), (0, 1), (0, 1)]$$

$$M_2 = [(0.8564, 0.01158), (0.8333, 0.00965), \\ (0.13702, 0.0724), (0.1417, 0.0568), \\ (0.9312, 0.01071), (0, 1), (0.8846, 0.03544)]$$

$$O = \begin{bmatrix} (0,1) & (0,1) & (0,1) & (0,1) & (1,0) & (0,1) & (0,1) \\ (0,1) & (0,1) & (0,1) & (0,1) & (0,1) & (1,0) & (0,1) \\ (0,1) & (0,1) & (0,1) & (0,1) & (0,1) & (0,1) & (0.95,0.025) \\ (0,1) & (0,1) & (0,1) & (0,1) & (0,1) & (0,1) & (0.95,0.025) \end{bmatrix}$$

TABLE 5. IEEE-39 node grid test results.

No.	Fault signal	Troubleshooting result		Failure analysis
		Method in this article	The method in [12]	
1	$L_{Sm25\text{-}26}$, $L_{Rm25\text{-}26}$, CB_3, CB_4	$L_{25\text{-}26}$: 0.9673	$L_{25\text{-}26}$: 0.9668	Normal
2	$L_{Sm25\text{-}26}$, $L_{Rm25\text{-}26}$, CB_3, $L_{Rs26\text{-}29}$, $L_{Rs26\text{-}27}$, $L_{Rs26\text{-}28}$, CB_6, CB_8, CB_{12}	$L_{25\text{-}26}$: 0.9879	$L_{25\text{-}26}$: 0.9601	CB_4 failed action
3	B_{1m}, $L_{Sp26\text{-}29}$, CB_5, CB_7, CB_2, $L_{Sm26\text{-}25}$, $L_{Rs26\text{-}25}$, $L_{Sm26\text{-}29}$, $L_{Rm29\text{-}26}$, CB_9, CB_6, CB_4	B_1: 0.9852; $L_{26\text{-}29}$: 0.9673; $L_{25\text{-}26}$: 0	B_1: 0.9516; $L_{26\text{-}29}$: 0.9668; $L_{25\text{-}26}$: 0	$L_{Sm26\text{-}25}$ and $L_{Sp26\text{-}29}$ mal operation; CB_3 failed action
4	$L_{Sm25\text{-}26}$, $L_{Rm25\text{-}26}$, $L_{Rs26\text{-}29}$, $L_{Rs26\text{-}27}$, $L_{Rs26\text{-}28}$, CB_6, CB_8, CB_{12}	$L_{25\text{-}26}$: 0.9879	$L_{25\text{-}26}$: 0.9385	CB_4 failed action; CB_3 information missing
5	$L_{Sm25\text{-}26}$, CB_3	$L_{25\text{-}26}$: 0.4836	$L_{25\text{-}26}$: 0.4316	$L_{Sm25\text{-}26}$ mal operation
6	$L_{Sm25\text{-}26}$,	$L_{25\text{-}26}$: 0	$L_{25\text{-}26}$: 0.1341	False information
7	T_{1p}, CB_1, CB_2	T_1: 0.9765	T_1: 0.9496	T_{1m} failed action

$$M_3 = [(0.8564, 0.01158), (0.8333, 0.00965), (0.13702, 0.0724), (0.1417, 0.0568), (0.9322, 0.01071), (0, 1), (0.8846, 0.03544)]$$

Because $M_3 = M_2$, the inference calculation ends, and the fault confidence of the T_1 direction is (0.8846, 0.03544). In the same calculation form, the fault confidence in both the $L_{25\text{-}2}$ direction and the $L_{25\text{-}26}$ direction are all (0.8846, 0.03544). The final failure probability value is: $f(B_1) = 0.9866$, $f(B_1) > \theta$, where B_1 is the faulty device.

In the process of matrix deduction, when the main protection of the Busbar is correctly operated, the corresponding transition of the backup protection cannot fire. Many calculations are omitted in the subsequent derivation of the matrix, which has considerable benefits when the network size is large enough. From the perspective of calculation speed, the arithmetic unit, and especially the multiplier, is one of the key Eq of the modern digital systems, which affects the efficiency of the whole system dramatically [24]. In this paper, taking the Busbar B_1 model as an example and taking the number of multiplication operations as the evaluation standard, the efficiency of the improved model can be increased by about 30%.

IV. ANALYSIS OF TYPICAL FAILURE CASES

A. SIMULATION CASE ANALYSIS

The effectiveness of the proposed method was verified by the simulation with the IEEE-39 node system. To verify the effectiveness of the proposed method in a complex information environment, the simulation cases used in this paper contain various common fault conditions, involving seven different fault cases and covering a variety of complex faults: single Eq fault, multi-element failure and loss of information, refusal or mis-operation, and confusion of information. The results show that compared with other power grid fault diagnosis methods, this method is more accurate for determining faulty Eq. The specific fault information, diagnosis results, and fault analysis are shown in Table 5.

TABLE 6. Real grid model fault signal.

No.	Fault information
1	Protection operation of over-current section I of Hou-Zhong line
2	#1 transformer medium-voltage side back-up protection act
3	Circuit breaker 100 opening
4	#2 transformer main protection start-up
5	Circuit breaker 202 opening
6	Circuit breaker 102 opening
7	Circuit breaker 302 opening

To further clarify the algorithm presented in this paper, take case No. 3 in Table 3 as an example for detailed fault analysis. This case is a complex failure that covers refusal and mis-operation. The alarm information for this fault is: {B_{1m}, $L_{SP26\text{-}29}$, CB_5, CB_7, CB_2, $L_{Sm26\text{-}25}$, B_{1s}, $L_{Sm26\text{-}29}$, $L_{Rm29\text{-}26}$, CB_9, CB_6, CB_4}.

According to the topology analysis, it is judged that the possible faulty elements are B_1, line $L_{26\text{-}29}$, and line $L_{25\text{-}26}$.

For Busbar B_1, the fault diagnosis model of the intuitionistic fuzzy Petri net with inhibitor arc is first established. The set satisfying the Busbar B_1 fault is {B_{1m}, CB2, CB_9, B_{1s}, CB_4}. After analysis, the circuit breaker CB_3 refuses to operate, and the fault spreads to the adjacent Eq $L_{25\text{-}26}$. Finally, the far backup protection of Busbar B_1 in the $L_{25\text{-}26}$ direction is triggered and the CB_4 is tripped, and the fault is removed.

The fault probability of the Busbar in the $L_{25\text{-}26}$ direction is calculated to be: $P(B_{1L25\text{-}26}) = 0.9825$, and the fault probability of the Busbar in the T_1 direction is: $P(B_{1T1}) = 0.9866$. For the Busbar in the $L_{25\text{-}2}$ direction, the probability of fault is: $P(B_{1L25\text{-}2}) = 0.9866$. The comprehensive fault probability value of Busbar B_1 is $P(B_1) = 0.9852 > \theta$, and Busbar B_1 fails.

For the line $L_{26\text{-}29}$, an intuitionistic fuzzy Petri net fault diagnosis model with inhibitor arc is established, and the fault set of the line $L_{26\text{-}29}$ is satisfied as {$L_{Sm26\text{-}29}$, CB_5, $L_{Rm29\text{-}26}$, CB_6, $L_{SP26\text{-}29}$}. After analysis, we found that the near backup

TABLE 7. Comparison of diagnostic results of real cases.

The suspected fault Eq	#2 Transformer		Hou-Zhong line		35KV Bus II	
	Method in [12]	Method in this article	Method in [12]	Method in this article	Method in [12]	Method in this article
Certainty degree	0.7280	0.8293	0.6221	0.7397	0.3608	0.2
Non-membership degree	0.0278	0.0094	0.0383	0.03347	0.3308	0.6
Failure probability	0.9618	0.9887	0.9384	0.9548	0.0831	0
Method in [7]	0.9684		0.5135		0.4401	

TABLE 8. Comparison of the methods in this paper with other existing methods.

Method	Information processing	Inferential calculation	Model characteristics
Method in [7]	Fuzzy processing	Simple matrix operations. All relevant libraries of faulty Eq are involved in the calculation.	Fuzzy petri net. When the network topology changes, it is necessary to re-model the faulty Eq and retrain the network.
Method in [9]	Fuzzy processing	Simple matrix operations. All relevant libraries of faulty Eq are involved in the calculation.	Layered fuzzy Petri net. The ability of the model to adapt to network topology changes is better, but the inference calculation process may fall into local extremum. Human factors have a stronger impact on the diagnosis results.
Method in [12]	Intuitionistic fuzzy processing	Simple matrix operations. All relevant libraries of faulty Eq are involved in the calculation.	Intuitionistic fuzzy petri net. When the network topology changes, it is necessary to re-model the faulty Eq and retrain the network. Human factors have a greater impact on the diagnosis results.
Method in this article	Intuitionistic fuzzy processing	Simple matrix operations. The Place that does not satisfy the model condition does not participate in the calculation, and the amount of calculation is greatly reduced.	Method of fault diagnosis using neural intuitionistic fuzzy Petri net with inhibitor arc. The adaptability of the model is better when the network topology changes. The troubleshooting speed is fast. Human factors have less impact on the diagnosis results.

protection $L_{SP26\text{-}29}$ of the transmitting end of line $L_{26\text{-}29}$ is malfunction. Because the main protection of the line and the corresponding circuit breaker are tripped, the near backup protection $L_{SP26\text{-}29}$ of the transmitting end cannot make the transition fire. The Eq in this direction does not participate in the probability calculation of the line $L_{26\text{-}29}$. The final failure probability of line $L_{26\text{-}29}$ is $P(L_{26\text{-}29}) = 0.9673 > \theta$, and line $L_{26\text{-}29}$ is faulty.

The set of faults satisfying line $L_{25\text{-}26}$ is $\{L_{Sm26\text{-}25}, CB_4\}$. Since CB_4 exists in the fault set of Busbar B_1 and meets the protection setting logic rules of the Busbar, the corresponding circuit breaker of $L_{Sm26\text{-}25}$ does not trip. The protection and circuit breakers associated with CB_4 are not tripped, so $L_{Sm26\text{-}25}$ can be judged to be malfunctioning, and the corresponding failure probability of the line can be calculated by the model to obtain $P(L_{Sm26\text{-}25}) = 0$.

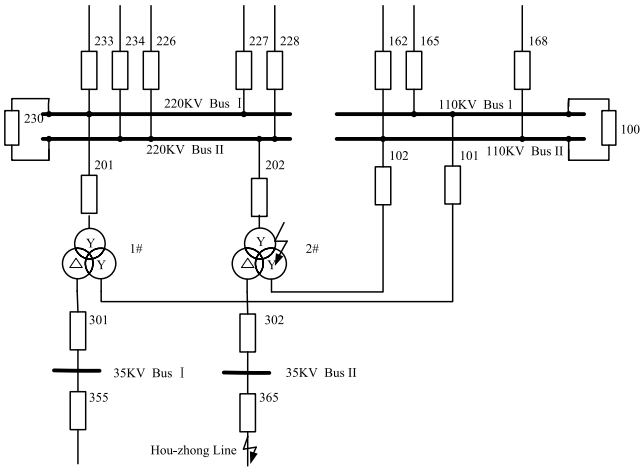

FIGURE 7. Real grid model diagram.

B. ACTUAL FAULT CASE ANALYSIS

The actual case involved a fault in the local network of the Hou-zhong line grid [12], as shown in Figure 7. The fault alarm information is shown in Table 6. To verify the effectiveness of the proposed method in the actual grid fault diagnosis, the control variable analysis method was used to analyze the fault, and only the fault diagnosis method was

compared using the same fault information and the same grid structure. The results show that the method developed in this study has advantages over the original method in terms of the accuracy of fault diagnosis, the non-membership degree, and the final fault probability. The detailed comparison information is shown in Table 7.

Table 8 compares the methods herein and the methods in the literature. The table shows that the algorithm logic is embedded in the model, which reduces the amount of calculation, improves the operation speed, and enhances the adaptability of the model. Through the intuitionistic fuzzy set, the Eq fault information is comprehensively considered from multiple dimensions (determination and non-membership degree), which improves the fault diagnosis accuracy. The neural network algorithm is used to train the weight parameters, which reduces the error in the fault diagnosis results caused by human factors. The model can also provide accurate and effective judgments under complex faults and failure of circuit breakers, mis-operation, loss of information, and information confusion.

V. CONCLUSION

In this study, we used intuitionistic fuzzy set was used in to deal with the uncertainty of the information present in grid fault diagnosis. The intuitionistic fuzzy set comprehensively considers the characteristics of the membership degree of the fault information and the non-membership characteristics, so the description of the uncertain information is more accurate and the accuracy of the calculated result is further improved. The BP algorithm is used to optimize the weight parameters of the model, which reduces the error caused by human factors on the fault diagnosis results.

To realize fast and real-time online power grid fault diagnosis, we introduced inhibitor arc tuple in the intuitionistic fuzzy Petri net model, and established a fault diagnosis model for intuitionistic fuzzy Petri net with inhibitor arc, which reduces unnecessary calculations and improves the speed of fault diagnosis.

The use of hierarchical transitions and Gaussian functions in the model reasoning process to optimize the inter-layer data improves the accuracy of the diagnostic results. The simulation of the example also shows that the diagnostic results after processing are more accurate. The above results confirm the effectiveness of the proposed method, but the application of multi-source information in power grid fault diagnosis needs further exploration.

APPENDIX

The IFIAPN model of line $L_{25\text{-}26}$ is shown in Figure 8. The subnet models of the fault propagation directions of the receiving end and the transmitting end are respectively shown in (1) and (2) of Figure 8, and the comprehensive diagnosis model is shown in (3) of Figure 8. Since the IFIAPN fault diagnosis model of the transformer is the same as the line, only the corresponding protection and circuit breaker are different and are not listed here.

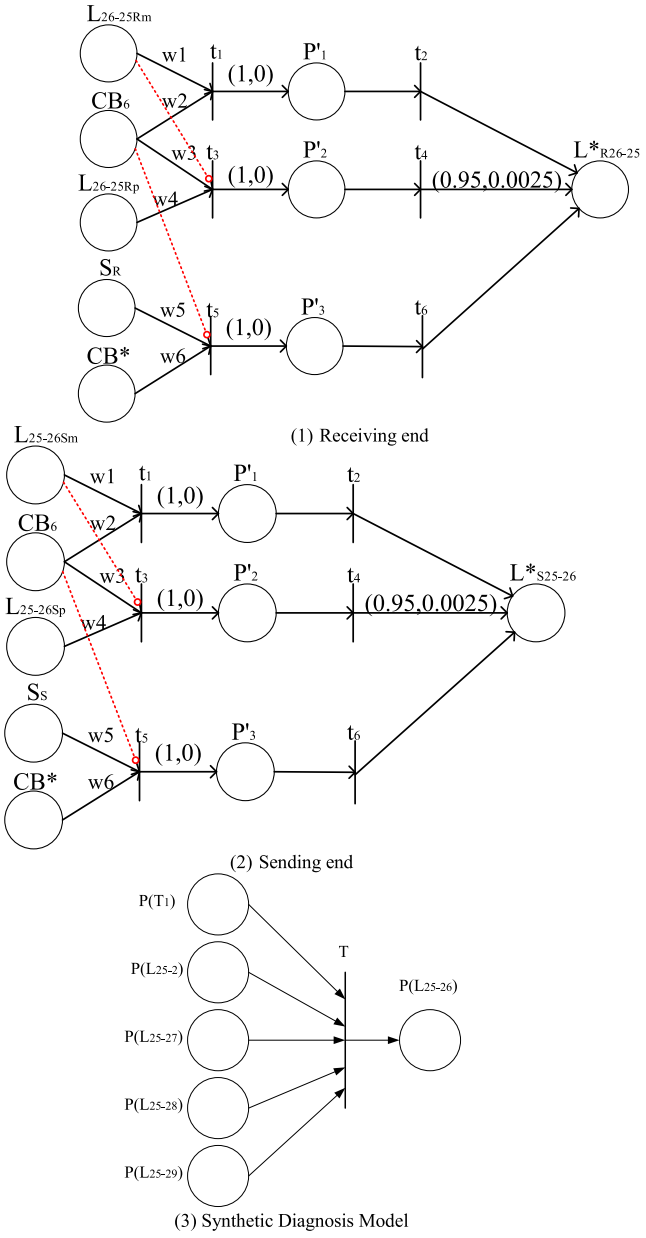

FIGURE 8. Petri net model of line $L_{25\text{-}2}$.

REFERENCES

[1] X. Bai, L. Qu, and W. Qiao, "Robust AC optimal power flow for power networks with wind power generation," *IEEE Trans. Power Syst.*, vol. 31, no. 5, pp. 4163–4164, Sep. 2016.

[2] D. Ma, Y. Liang, X. Zhao, R. Guan, and X. Shi, "Multi-BP expert system for fault diagnosis of powersystem," *Eng. Appl. Artif. Intell.*, vol. 26, no. 3, pp. 937–944, 2013.

[3] Z. Yongli, H. Limin, and L. Jinling, "Bayesian networks-based approach for power systems fault diagnosis," *IEEE Trans. Power Del.*, vol. 21, no. 2, pp. 634–639, Apr. 2006.

[4] A. F. Novelo, E. Q. Cucarella, E. G. Moreno, and F. M. Anglada, "Fault diagnosis of electric transmission lines using modular neural networks," *IEEE Latin Amer. Trans.*, vol. 14, no. 8, pp. 3663–3668, Aug. 2016.

[5] M. Noori, R. Effatnejad, and P. Hajihosseini, "Using dissolved gas analysis results to detect and isolate the internal faults of power transformers by applying a fuzzy logic method," *IET Gener., Transmiss. Distrib.*, vol. 11, no. 10, pp. 2721–2729, 2017.

[6] V. Calderaro, C. N. Hadjicostis, A. Piccolo, and P. Siano, "Failure identification in smart grids based on petri net modeling," *IEEE Trans. Ind. Electron.*, vol. 58, no. 10, pp. 4613–4623, Oct. 2011.
[7] Y. Dong, J. Zhang, Z. Li, Y. Hu, and Y. Deng, "Combination of evidential sensor reports with distance function and belief entropy in fault diagnosis," *Int. J. Comput. Commun. Control*, vol. 14, no. 3, pp. 329–343, 2019.
[8] J. Yang, Z. He, and T. Zang, "Power system fault-diagnosis method based on directional weighted fuzzy Petri nets," *Proc. Chin. Soc. Elect. Eng.*, vol. 30, no. 34, pp. 42–49, 2010.
[9] H. Xie and X. Tong, "A method of synthetical fault diagnosis for power system based on fuzzy hierarchical Petri net," *Power Syst. Technol.*, vol. 36, no. 1, pp. 247–252, 2012.
[10] R. Li and X. Qiu, "Improvement in fault diagnosis of transmission networks using fuzzy Petri net," *Electr. Power*, vol. 41, no. 5, pp. 50–54, 2008.
[11] J. Sun, S.-Y. Qin, and Y.-H. Song, "Fault diagnosis of electric power systems based on fuzzy Petri nets," *IEEE Trans. Power Syst.*, vol. 19, no. 4, pp. 2053–2059, Nov. 2004.
[12] X. Zhang, S. Yue, and X. Zha, "Method of power grid fault diagnosis using intuitionistic fuzzy Petri net," *IET Gener., Transmiss. Distrib.*, vol. 12, no. 2, pp. 295–302, Jan. 2018.
[13] M. Tan, J. Li, X. Chen, and X. Cheng, "Power grid fault diagnosis method using intuitionistic fuzzy Petri nets based on time series matching," *Complexity*, vol. 2019, Jul. 2019, Art. no. 7890652.
[14] H. Zhang and Y. Deng, "Engine fault diagnosis based on sensor data fusion considering information quality and evidence theory," *Adv. Mech. Eng.*, vol. 10, pp. 1–10, Nov. 2018.
[15] H. Zhang and Y. Deng, "Weighted belief function of sensor data fusion in engine fault diagnosis," in *Soft Computing*. Berlin, Germany: Springer, May 2019, pp. 1–11. doi: 10.1007/s00500-019-04063-7.
[16] J. Li, X. Zhu, and X. Cheng, "Sensor fault diagnosis based on fuzzy neural Petri net," *Complexity*, vol. 2018, Oct. 2018, Art. no. 8261549.
[17] L. C. Jain, "Neural architectures of fuzzy Petri nets," in *Recent Advances in Artificial Neural Networks*. Boca Raton, FL, USA: CRC Press, 2018, pp. 341–368.
[18] L. Fei, H. Wang, L. Chen, and Y. Deng, "A new vector valued similarity measure for intuitionistic fuzzy sets based on owa operators," *Iranian J. Fuzzy Syst.*, vol. 16, no. 3, pp. 113–126, 2019.
[19] H.-C. Liu, J.-X. You, X.-Y. You, and Q. Su, "Fuzzy Petri nets using intuitionistic fuzzy sets and ordered weighted averaging operators," *IEEE Trans. Cybern.*, vol. 46, no. 8, pp. 1839–1850, Aug. 2016.
[20] X. Cong, Y. Chen, Z. Li, N. Wu, E. A. Nasr, and A. M. El-Tamimi, "Optimal Petri net supervisors of discrete event systems via weighted and data inhibitor arcs," *IEEE Access*, vol. 6, pp. 8245–8257, 2018.
[21] Q. Su, F. He, N. Wu, and Z. Lin, "A method for construction of software protection technology application sequence based on Petri net with inhibitor arcs," *IEEE Access*, vol. 6, pp. 11988–12000, 2018.
[22] Y. Zhou, Y. Wang, and M. Zhao, "The operation of national grid relay protection and safety automatic devices in 2004," *Power Syst. Technol.*, vol. 16, pp. 42–48, 2005.
[23] L. Zhang, D. Wang, Y. Liu, Z. Zhou, P. Lu, Z. Wang, W. Li, Y. Liu, H. Shen, and G. Yang, "Analysis of the operation of 220 kV and above AC protection in the national grid," *Power Syst. Technol.*, vol. 41, no. 5, pp. 1654–1659, 2017.
[24] A. He, X. Liu, and H. Chen, "Design of 8-bit asynchronous booth multiplier based on constrained data bundled two-phase handshake protocol," *Chin. J. Electron.*, vol. 46, no. 4, pp. 961–968, 2018.

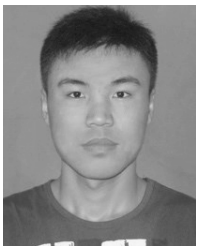

MINGYUE TAN is currently pursuing the master's degree with the Department of the Electrical Engineering and Automation, Shandong University of Science and Technology. His research interests include automation of electric power systems and power system fault diagnosis.

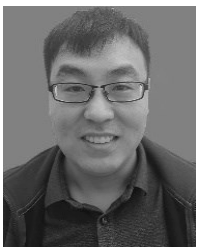

JIMING LI is currently pursuing the Ph.D. degree with the Department of the Electrical Engineering and Automation, Shandong University of Science and Technology. His research interests include signal processing, inspection technology, and system integration.

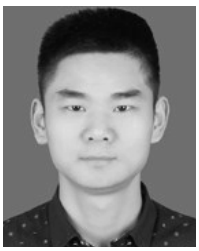

GUANGYUAN XU is currently pursuing the master's degree with the Department of the Electrical Engineering and Automation, Shandong University of Science and Technology. His research interests include automation of electric power systems and power system fault diagnosis.

XUEZHEN CHENG is currently a Professor with the Department of the Electrical Engineering and Automation, Shandong University of Science and Technology, Qingdao, China, where she is also the Director of the Automation Department. Her research interests include power system automation, inspection technology and system integration, and information and image processing. She has led and participated in more than ten research projects at the national and provincial levels. She is also a China Postdoctoral Fund Committee Project Reviewer and a China Energy Society Expert.